IC/94/337
INTERNAL REPORT
(Limited Distribution)

International Atomic Energy Agency
and
United Nations Educational Scientific and Cultural Organization
INTERNATIONAL CENTRE FOR THEORETICAL PHYSICS

SPECTRAL RESPONSE OF A POLYCRYSTALLINE SILICON SOLARCELL

B. Ba [1]
International Centre for Theoretical Physics, Trieste, Italy

and

M. Kane
Laboratoire des Semi–conducteurs et d'Energie Solaire,
Faculteé des Sciences et Techniques, Université Cheikh Anta Diop,
Dakar, Sénégal.

ABSTRACT

A theoretical study of the spectral response of a polycrystalline silicon n-p junction solar cell is presented. The case of a fibrously oriented grain structure, involving grain boundary recombination velocity and grain size effects is discussed. The contribution of the base region on the internal quantum efficiency Q_{int} is computed for different grain sizes and grain boundary recombination velocities in order to examine their influence. Suggestions are also made for the determination of base diffusion length in polycrystalline silicon solar cells using the spectral response method.

MIRAMARE - TRIESTE

October 1994

[1]Permanent address: Laboratoire des Semi–conducteurs et d'Energie Solaire, Faculté des Sciences et Techniques, Université Cheikh Anta Diop, Dakar, Sénégal.

1 Introduction

Various optical methods for the characterization of solar cells are available in the literature [1–7]. Among them, the spectral response measurements are made in order to understand the photovoltaic behaviour of these devices and to extract some key parameter like base minority carriers diffusion length. The studies deal in general with single-crystal cells for which the experimental data are interpreted using a one-dimensional theory. In polycrystalline silicon solar cells, because of the presence of numerous grains relatively ordered in fibrous or random orientation, the three-dimensional model [8–10] is more suitable for the resolution of the minority carrier diffusion equation with more than two boundary conditions. In this paper, this approach is used in order to investigate the spectral response of a polycrystalline n-p junction silicon solar cell. By means of numerical simulations, the influence of the grain size, the grain boundary recombination velocity and the base minority diffusion length on the contribution of the base region on the internal quantum efficiency are examined.

2 Theory

The calculations are performed using results already obtained and recently published [10]. The polycrystalline solar cell is considered as an array of parallelepipedic grains bounded by regions acting as minority carriers sinks (grain boundaries) perpendicular to the junction. Their electrical activity is described by a grain boundary recombination velocity S_{ng}. It is assumed a uniform doping of the n (emitter) and p (base) regions (i.e constant bulk parameters: lifetime, diffusion length etc.). It is also considered that no electric field effect occurs inside the base region so that carrier transport is effected only by diffusion.

The internal quantum efficiency Q_{int} is the number of electron-hole pairs collected at each wavelength relative to the number of photons entering the material at that

wavelength.

$$Q_{int} = \frac{I_{sc}}{q\, F_0(\lambda)\, (1 - R_\lambda)} \tag{1}$$

The reflection coefficient R_λ depends on the wavelength λ of the incident monochromatic photons flux $F_0(\lambda)$ falling normally to the n-type front surface of the cell. I_{sc} is the steady-state base photocurrent flowing out of the base region into the space charge region:

$$\begin{aligned} I_{sc} &= q\, \alpha_\lambda\, (1 - R_\lambda)\, F_0(\lambda)\, \exp[-\alpha_\lambda (z_e + W)] \sum_{i=1}^{\infty} \sum_{j=1}^{\infty} \sum_{k=1}^{\infty} \frac{C_{ij}\, L_{ijk}^2\, \mu_k^2\, A_{\mu_k}^2}{(\alpha_\lambda^2 + \mu_k^2)} \\ &\times \left[1 - \left(1 - \frac{S_n}{\alpha_\lambda\, D_n} \right) \frac{\alpha_\lambda\, sin\,(\mu_k H_b)\, \exp(-\alpha_\lambda H_b)}{\mu_k} \right] \end{aligned} \tag{2}$$

with

$$C_{ij} = \frac{4\, A_{k_i}^2\, sin^2(k_i a)\, A_{l_j}^2\, sin^2(l_j b)}{k_i^2\, l_j^2\, a\, b} \tag{3}$$

and

$$L_{ijk} = \left(\frac{1}{L_n^2} + k_i^2 + l_j^2 + \mu_k^2 \right)^{-1/2} \tag{4}$$

The procedure to find the expression of I_{sc} and the quantities k_i, l_j, μ_k, A_{k_i}, A_{l_j}, A_{μ_k}, is given in previous works [10, 11]. The dimensions of each grain in x and y directions are respectively $2a$, and $2b$. For simplicity a square section for grains is considered (i.e the grain size is $X_g = 2a = 2b$ and the grain boundary recombination velocity in the base region S_{ng} is the same in x and y-directions. The emitter thickness is z_e, the junction depth is W and $H_b = H - (z_e + W)$ is the thickness of the p-type base region, H being the cell thickness.

3 Results and discussions

The computer simulations are carried out in the case of a back surface field solar cell [12] (i.e the back surface recombination velocity is $S_n = 0$). The emitter and the cell thicknesses are respectively $z_e = 0.5\mu m$ and $H = 200\mu m$. The value of W and the bulk parameters of the cell like the minority carrier diffusion length L_n and the diffusion coefficient D_n for electrons in the base, are taken from [13].

The "internal" spectral response of a polycrystalline silicon solar cell is displayed in Fig.1 with, for comparison, that of a single-crystal n-p junction solar cell developed by Hovel [13]. Fig.1 shows the effects of varying the grain size (X_g = 1, 10, 100 and $1000\mu m$), while keeping the grain boundary recombination velocity constant ($S_{ng} = 100m/s$). It is observed that the peak response shifts to longer wavelengths as the grain size increases. It is also seen that the grain size has no influence on the quantum efficiency in short wavelengths range ($\lambda < 0.5\mu m$) corresponding to the generation of excess minority carriers in a thin layer at the surface because of high absorption coefficient for silicon. On the contrary, long wavelength light is deeply absorbed and since no recombination takes place at the back contact ($S_n = 0$), the grain size effects become important. Small grained cells have lower quantum efficiencies in long wavelength range while large grained cells ($X_g > 1000\mu m$) tend to the single-crystal behaviour.

Fig.2 displays the internal quantum efficiency in a $100\mu m$ grain size cell with S_{ng} taking the values 0, 10, 100, 10^3 and $10^4 m/s$. It is observed that the grain boundary recombination velocity has no effect in the short wavelength part of the quantum efficiency. When S_{ng} decreases, the quantum efficiency at longer wavelength is increased due to small recombination in grain boundaries. For solar cells with no grain boundary activity ($S_{ng} = 0$), the spectral response is mainly governed by recombination loss in the bulk region. This is illustrated in Fig.3 where three values of the base diffusion length: L_n = 52.2, 164 and $232\mu m$ are considered in the case of a $100\mu m$ grain size cell. If L_n increases, the internal quantum efficiency increases and

the peak response moves toward the longer wavelengths. On the contrary, in the polycrystalline cell with high value of S_{ng} ($10^4 m/s$), an increase in the base diffusion length, increases the influence of grain boundary recombinations and then reduces the spectral response of the cell.

The plots of the inverse of the internal quantum efficiency Q_{int}^{-1} against the reciprocal of absorption coefficient α_λ^{-1} are shown in Fig.4. They concern a cell with moderate grain boundary activity ($S_{ng} = 1m/s$) at different grain sizes. A bulk diffusion length $L_n = 52.5\mu m$ is chosen so that the ratio $H/L_n > 2.5$ is respected which is required for an accurate determination of the solar cells base diffusion length using photoresponse methods [3, 4]. The plots are linear curves for λ values between 0.90 and $1.05\mu m$. The intercepts obtained by the extrapolation of these linear parts with the α_λ^{-1}-axis, give the absolute values: 38, 51.5 and $53.7\mu m$ respectively for the following grain sizes: $10\mu m$, $100\mu m$ and $1000\mu m$. A value close to L_n is obtained for the large grain size with an error of about 1.4% for $X_g = 100\mu m$ and 3% for $X_g = 1000\mu m$. This precision can be improved by summing over a great number of terms k_i and l_j since for great values of X_g and S_{ng}, the series giving the photocurrent are slowly converging [14]. For small grained cell, the series are quickly converging if the summation over k_i and l_j terms is considered. The pseudo diffusion length $\gamma_{n_{ij}} = L_n/\sqrt{(1 + L_n^2(k_i^2 + l_j^2)}$ [8], associated to the grain effects and calculated using only the first order terms k_1 and l_1 is $36.9\mu m$. This value is very close to the one of the intercept for $X_g = 10\mu m$ and indicates the predominance of grain boundaries activity on the spectral response of the cell.

However, the spectral response method gives only a value of the base diffusion length averaged over a large volume of the cell. Since, a polycrystalline silicon solar cell contains a relatively large number of structural imperfections (dislocations, grains boundaries, etc.) a better spatial resolution for the determination of the local diffusion length can be obtained by scanning light or electron beam induced current techniques [15].

4 Conclusions

In this work, the grain effects on spectral response in a polycrystalline silicon solar cell are examined. The base region contribution of weakly doped cell is strongly dependent on the grain size and grain boundary recombination velocity in long wavelengths range.

Acknowledgments

One of the authors (B.B.) would like to thank Professor Abdus Salam, the International Atomic Agency and UNESCO for hospitality at the International Centre for Theoretical Physics, Trieste. He also expresses his deep sense of gratitude to the Swedish Agency for Research Cooperation with Developing Countries (SAREC) for financial support during his visit at the ICTP under the Associateship scheme.

References

[1] J. S. HARTMAN and M. A. LIND, Sol. Cells **7**, 147 (1982/83).

[2] T. L. CHU, E. D. STOKES and S. S. CHU, Sol. Cells **1**, 222 (1979/1980).

[3] N. D. ARORA, S. G. CHAMBERLAIN and D. J. ROULSTON, Appl. Phys. Lett. **37**, 325 (1980).

[4] P. K. BASU, S. N. SINGH. N. K. ARORA and B. C. CHAKRAVARTY, IEEE Trans. Electrons Devices **41**, 367 (1994).

[5] O. VON ROOS, J. appl. Phys. **51**, 1852 (1980).

[6] N. CONVERS WYETH and A. CATALANO, J. appl. Phys. **50**, 1403 (1979).

[7] J. LAGOWSKI, A. M. KONTKIEWICZ, L. JASTRZEBSKI and P. EDELMAN, Appl. Phys. Lett. **63**, 2902 (1993).

[8] N. C. HALDER and T. R. WILLIAMS, Sol. Cells **11**, 201 (1982).

[9] S. ELNAHAWY and N. ADEEB, Solid State Electronics **33**, 169 (1990)

[10] B. BA, M. KANE, A. FICKOU and G. SISSOKO, Sol. Ener. Mat. and Sol. Cells **31**, 33 (1993).

[11] B. BA, These de 3eme Cycle, Faculté des Sciences et Techniques, Dakar, Sénégal, (Dec 1991).

[12] O. VON ROOS, J. appl. Phys. **49**, 3503 (1978).

[13] H. J. HOVEL, Semiconductors and Semimetals, Vol 11, Solar Cells (Academic Press, New York, 1975).

[14] S. C. JAIN, R. JANSSENS, G. CHEEK, P. DEPAUW, R. MERTENS and R. VAN OVERSTRAETEN, Sol. Cells **9**, 345 (1983).

[15] C. DONOLATO, J. appl. Phys. **54**, 1314 (1983).

Figure captions

Fig.1: Computed internal quantum efficiency of the base region for various grain sizes. $S_{ng} = 100m/s$; $L_n = 52.2\mu m$.

Fig.2: Computed internal quantum efficiency of the base region for various grain boundary recombination velocities. $X_g = 100\mu m$; $L_n = 52.2\mu m$.

Fig.3: Computed internal quantum efficiency of the base region for various base diffusion lengths. $X_g = 100\mu m$; $S_{ng} = 0$ and $10^4 m/s$.

Fig.4: Reciprocal of the internal quantum efficiency of the base region versus the inverse of absorption coefficient for three values of the grain size. $S_{ng} = 1m/s$.

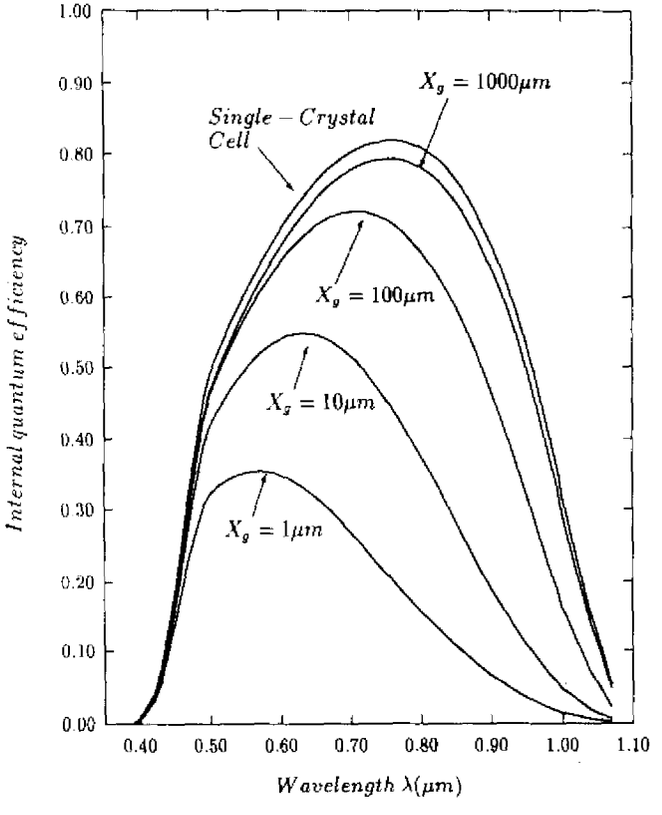
1.00
0.90
0.80
0.70
0.60
0.50
0.40
0.30
0.20
0.10
0.00
0.40
0.50
0.60
0.70
0.80
0.90
1.00
1.10
Internal quantum efficiency
Wavelength λ(μm)
Single − Crystal Cell
$X_g = 1000\mu m$
$X_g = 100\mu m$
$X_g = 10\mu m$
$X_g = 1\mu m$

Fig.1

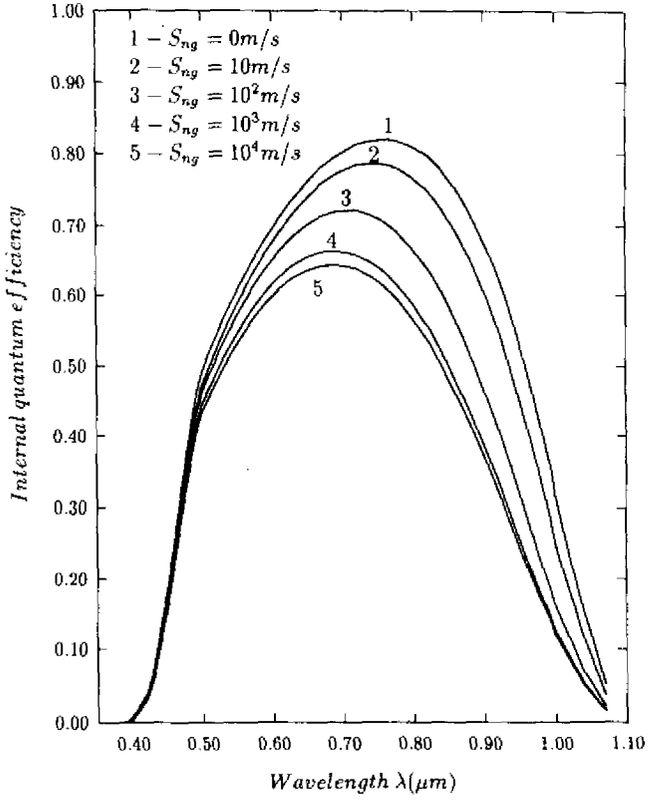
1.00
0.90
0.80
0.70
0.60
0.50
0.40
0.30
0.20
0.10
0.00
0.40
0.50
0.60
0.70
0.80
0.90
1.00
1.10
Internal quantum efficiency
Wavelength λ(μm)
$1 - S_{ng} = 0m/s$
$2 - S_{ng} = 10m/s$
$3 - S_{ng} = 10^2m/s$
$4 - S_{ng} = 10^3m/s$
$5 - S_{ng} = 10^4m/s$
1
2
3
4
5

Fig.2

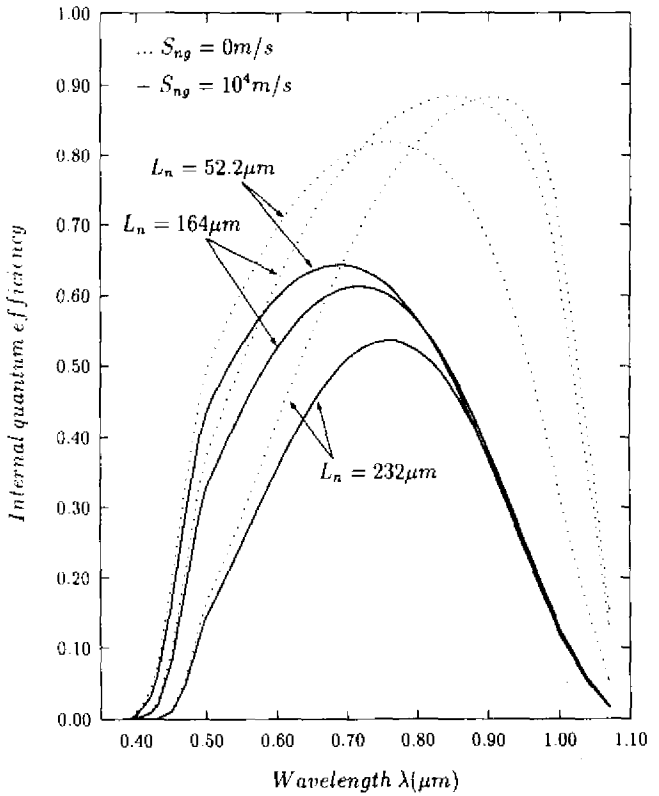
... $S_{ng} = 0m/s$
– $S_{ng} = 10^4 m/s$
$L_n = 52.2\mu m$
$L_n = 164\mu m$
$L_n = 232\mu m$
Internal quantum efficiency
Wavelength $\lambda(\mu m)$
1.00
0.90
0.80
0.70
0.60
0.50
0.40
0.30
0.20
0.10
0.00
0.40
0.50
0.60
0.70
0.80
0.90
1.00
1.10

Fig.3

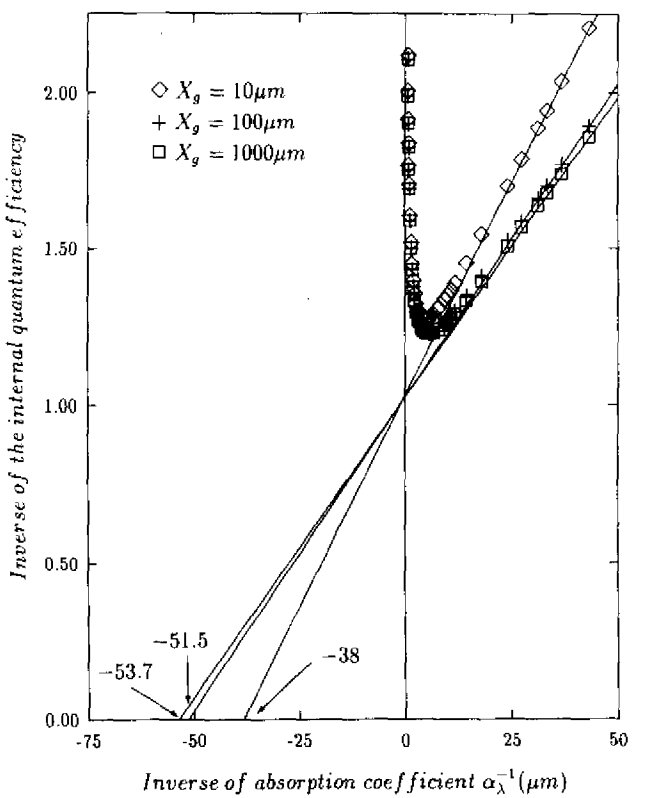
◇ $X_g = 10\mu m$
+ $X_g = 100\mu m$
□ $X_g = 1000\mu m$
−51.5
−53.7
−38
Inverse of the internal quantum efficiency
Inverse of absorption coefficient $\alpha_\lambda^{-1}(\mu m)$
2.00
1.50
1.00
0.50
0.00
-75
-50
-25
0
25
50

Fig.4